Separation and Reconstruction of the Rigid Body and Micro-Doppler Signal in ISAR Part II – Statistical Analysis

L. Stanković[1], S. Stanković[1], T. Thayaparan[2], M. Daković[1], I. Orović[1]

Abstract

Micro-Doppler effect corresponds to non-stationary components in the time-frequency domain, while the rigid body can be considered as a stationary signal during the processing time. This property is used in the first part of the paper to present the method for separation recovery based on the compressive sensing theory. Recovery bounds are based on the restricted isometry property or the coherence and spark analysis. Their calculation is a computationally difficult (NP hard) problem. These bounds also produce very pessimistic results. It is the reason to consider the statistical analysis of the reconstruction results. The statistical approach is presented in this part of the paper and illustrated by examples, including a detailed case study example.

I. Introduction

In the first part of this two-part paper, the micro-Doppler effects [1] and possibility of their separation from the rigid body in ISAR are considered [2]. The rigid body components behave as stationary within the coherence integration time [1], [3]–[6], while micro-Doppler components [4], [7] are non-stationary and well-concentrated in the time-frequency domain [8]–[10]. A time-frequency method for their separation is presented in [11], [12]. The removal of the overlapping parts of the micro-Doppler and rigid body components results in a reduced number of samples representing rigid body part of the signal. The sparsity property of the rigid body signal in the Fourier domain has indicated a possibility of reconstruction within the compressive sensing (CS) framework [13]. The compressive sensing reconstruction bounds are based on the restricted isometry property and coherence index analysis. They are quite conservative for engineering applications [14], [15]. One example illustrating this fact is presented in the Appendix. It was the main motivation for a statistical approach, presented in this part of the paper. The statistical approach is illustrated in a case study example. It shows that the full recovery results may be expected with high probability, well bellow the theoretical bounds.

The paper is organized as follows. In Section II a statistical comparison of the recovery in the time, frequency, and the joint time-frequency domain is done. A case study analysis is performed in Section III. The importance of the statistical analysis is highlighted on a simple example in Appendix.

[1] Ljubiša Stanković, Srdjan Stanković, Miloš Daković, and Irena Orović are with University of Montenegro, Faculty of Electrical Engineering, 81000 Podgorica, Montenegro, E-mail: {ljubisa,srdjan,milos,irenao}@ac.me.

[2] Thayananthan Thayaparan is with Radar Applications and Space Technologies, Defence R&D Canada – Ottawa, Ottawa, Ontario, Canada, E-mail: Thayananthan.Thayaparan@drdc-rddc.gc.ca.

This research is supported by the Montenegro Ministry of Science project CS-ICT (Grant No. 01-1002).

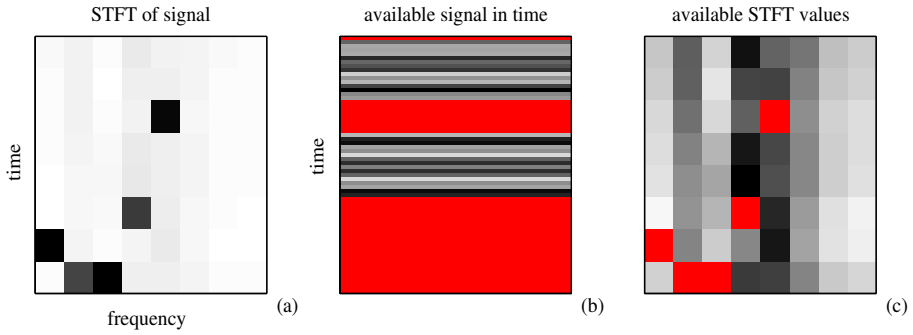

Fig. 1. (a) Time-frequency representation of a rigid body signal with nonstationary micro-Doppler disturbances. (b) Signal samples in the time domain with disturbed values being marked in red. (c) Signal samples in the time-frequency domain with disturbed values being marked in red.

II. Statistical Analysis

The reconstruction algorithm presented in the first part (of this two-part paper) is based on the rigid body frequencies estimation [15]. This calculation is done using the L-statistics to obtain the initial representation. The available samples are used to reconstruct the signal. The missing values are assumed to be zero. The initial estimation is based on the norm-two solution of the problem (norm-two solution is not sparse in the transformation domain). Initial position estimate plays the crucial role in these kind of algorithms. The initial estimate is related to the energy of the available measurements. Increasing the number of removed STFT values will degrade this estimate and possibility to reconstruct the signal. This fact is used in the restricted isometry property as well. The exact bounds calculation based on the restricted isometry property or the coherence and spark is a computationally very difficult (NP hard) problem. Even if these bounds are calculated, they give very pessimistic estimates of the parameters (see Appendix). This is the reason to consider the statistical analysis of the reconstruction results.

As an introduction to the analysis that follows let us observe an illustrative example. Assume a well localized nonstationary signal corresponding to micro-Doppler effect within five STFT values, as in Fig.1 (a). In general, this kind of nonstationary signal covers much larger percentage of signal samples in the time domain Fig.1 (b). When a single well localized time-frequency component exists in the time-frequency domain, it is usually present in several samples in the time domain. If these well localized nonstationary parts are removed in the time-frequency domain then we deal with the problem of a small percent of missing values in this domain, Fig.1 (c). Corresponding number of samples in the time domain will be analyzed next. Assume that well localized nonstationary signal appears randomly in several time-frequency regions.

The STFT of signal $x(n)$ whose length is N is calculated using M samples window, as explained in detail in [15]. Along frequency axis there will be M columns corresponding to frequencies resulting from one STFT calculation

$$\mathbf{STFT}_M(n) = \mathbf{W}_M \mathbf{x}(n)$$

where $\mathbf{x}(n)$ is signal vector with elements $\mathbf{x}(n)$=$[x(n), x(n+1), ..., x(n+M-1)]^T$ and and $\mathbf{W}_M$ is the $M \times M$ discrete Fourier transform (DFT) matrix with coefficients $W(m,k) = \exp(-j2\pi km/M)$.

The whole STFT column matrix $\mathbf{STFT}$ consists of stacked columns $\mathbf{STFT}_M(n)$ calculated for all $n = 0, M, 2M, ..., N-M$ in nonoverlapping case. Matrix $\mathbf{S}$ has the same values as the STFT column matrix of denoted by $\mathbf{STFT}$, but relocated in a matrix form to correspond the time-frequency plane location. Each point in the time frequency plane in this case will be represented by values $STFT(n,k)$. In the time direction, there are N/M rows corresponds to the time instants $n = 0, M, 2M, ..., N-M$ where the nonoverlapping STFT is calculated. In the nonoverlapping case dimension of $\mathbf{S}$ is $M \times (N/M)$. Assume that Q

of randomly positioned STFT values contain signal values $x(n)$ where the rigid body signal $x_{rb}(n)$ overlaps with the micro-Doppler components $x_{mD}(n)$. These are undesirable STFT and should be removed from the analysis. The remaining number of STFT values is $N_A = N - Q$ in the nonoverlapping STFT calculation.

Components of the signal $x(n)$ corresponding to the rigid body are modeled by

$$x_{rb}(n) = \sum_{i=1}^{K} \rho_i e^{j2\pi k_{0i} n/N} \tag{1}$$

at the cross-range positions (corresponding to the signal frequencies k_{0i}).

First we will calculate the number of time instants (denoted by e_Q) where all values (rows) of the matrix $\mathbf{S}$ are not disturbed. In these instants, the signal values used for STFT calculation are not disturbed as well. The problem will be solved in a recursive manner. If the number of STFT disturbed values is $Q = 0$, then obviously the number of undisturbed STFT rows is $e_0 = N/M$. For $Q = 1$, we easily get $e_1 = N/M - 1$ since only the STFT row where this disturbed STFT sample is located is disturbed. Let us denote the expected number of undisturbed rows for $Q = p$ by e_p. In order to find e_{p+1}, consider two possible cases:

1. The newly added disturbed STFT value is in the row where already exist disturbed STFT values. Then the number of undisturbed rows remains the same. Probability of this event is

$$P_I = \frac{N - e_p M - p}{N - p}$$

2. The disturbed value is added to the row with no disturbed values so far. In this case, the number of undisturbed rows is reduced by 1. Probability of this event is

$$P_{II} = \frac{e_p M}{N - p}.$$

Since these two events are mutually exclusive we have

$$e_{p+1} = e_p P_I + (e_p - 1) P_{II} = e_p \left(1 - \frac{M}{N - p}\right)$$

It means that the resulting e_Q is:

$$\begin{aligned} e_Q &= e_{Q-1} \left(1 - \frac{M}{N - (Q-1)}\right) \\ &= e_{Q-2} \left(1 - \frac{M}{N - (Q-2)}\right) \left(1 - \frac{M}{N - (Q-1)}\right) \\ &\dots \\ &= e_0 \left(1 - \frac{M}{N - 0}\right) \cdots \left(1 - \frac{M}{N - (Q-2)}\right) \left(1 - \frac{M}{N - (Q-1)}\right). \end{aligned}$$

Finally

$$e_Q = \frac{N}{M} \prod_{p=0}^{Q-1} \left(1 - \frac{M}{N - p}\right). \tag{2}$$

The number of undisturbed rows in the STFT can be easily related to the number of undisturbed signal samples in the time domain. For the STFT calculated without overlapping for each STFT column M signal samples are used in the calculation. If e_Q is the number of undisturbed rows then the number of undisturbed samples in time domain is

$$N_A = M\, e_Q = N \prod_{p=0}^{Q-1} \left(1 - \frac{M}{N - p}\right)$$

The above results presented by (2) are statistically checked. For various values of N, M and Q, the number of undisturbed samples is calculated by (2) and compared with statistical results. The results are shown in Table I for $N/M = 128$ and

TABLE I

STATISTICAL CHECK OF (2) FOR $N/M = 128$ AND $M = 32$. THE EXACT VALUE, THE STATISTICAL VALUE AND THE ERROR ARE SHOWN.

Q	Exact	Statistical	Error (%)
50	86.2713	86.2503	0.001
100	57.8607	57.8603	0.001
150	38.6108	38.6160	-0.014
200	25.6321	25.6136	-0.006
300	11.1161	11.1189	-0.025
500	1.9524	1.9527	-0.015

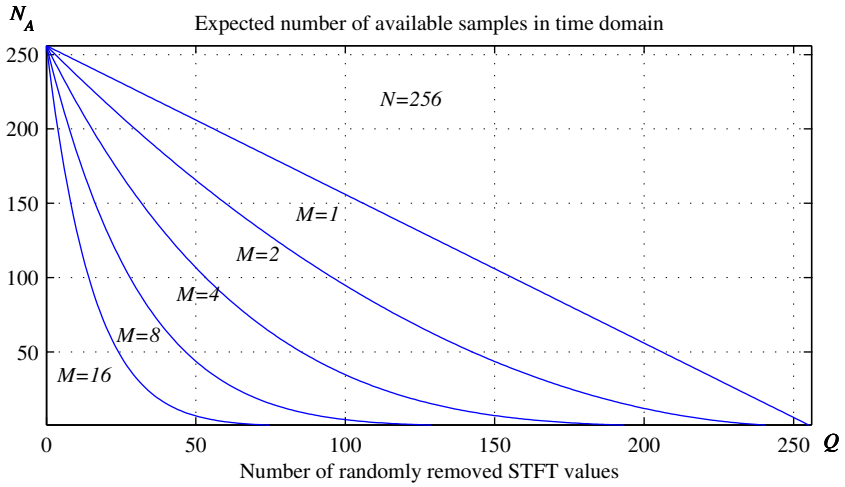

Fig. 2. Expected number of removed samples in time domain as a function of the number of disturbed and removed time-frequency values for $N = 256$ and various window lengths M in the STFT calculation.

$M = 32$. In each case, 10^6 random realizations are formed for $Q = 50, 100, 150, 200, 300, 500$. For a large number Q of disturbed STFT values the probability that a row is undisturbed is very small. In order to correctly estimate low probability event a large number of realization should be used. Expected number of available samples as a function of the number of disturbed samples Q for $N = 256$ and different M is presented in Fig.2.

Analysis of the signal and DFT can be obtained as a special case of the STFT analysis. Namely, with $M = 1$ the STFT reduces to the signal itself, $STFT(n, k) = x_{rb}(n)$. This case is already presented and studied in details in [12]. The time-frequency form presented in this section is used in [13] to separate the stationary sparse part of the signal from a strong impulsive noise disturbance. The analysis that follows will start from the special case when $M = 1$, meaning $\mathbf{STFT} = \mathbf{x}$ and $\mathbf{STFT}_{CS} = \mathbf{y}$, where $y(n)$ are available samples of $x_{rb}(n)$, $n \in \mathbb{N}_A$ and $\mathbf{x}$ is the vector with elements $x_{rb}(n)$. This is the case when the signal is analyzed in the time domain. It is studied in detail in [12]. For $M = 1$, the initial estimate of the Fourier transform of the rigid body is the solution of the norm-two minimization problem

$$\min \|\mathbf{X}\|_2 \text{ subject to } \mathbf{AX} = \mathbf{y} = \mathbf{STFT}_{CS},$$

where the measurement matrix $\mathbf{A}$ corresponds to the available samples.

This solution is quite simple for the DFT matrix. It will be denoted by $\mathbf{X}_2$ and its values by $X_2(k)$. Since Parseval's theorem holds then

$$\|\mathbf{X}\|_2 = \|\mathbf{x}\|_2$$

and the problem reduces to

$$\min \|\mathbf{x}\|_2 \text{ subject to } \mathbf{AX} = \mathbf{y}.$$

Since we have N_A fixed and given by the condition $\mathbf{AX} = \mathbf{y}$ then obviously $\|\mathbf{x}\|_2 = \sqrt{\sum_{n=0}^{N-1} |x_{rb}(n)|^2}$ is minimal if all unavailable signal samples (STFT with $M = 1$) are zero-valued. Therefore, the initial estimate of the rigid body DFT is

$$X_2(k) = N_A \underset{n \in \mathbb{N}_A}{\text{mean}} \{x_{rb}(n) e^{j2\pi kn/N}\}$$

The average value of $X_2(k)$ for signal $x_{rb}(n)$, assuming the integer values of k_{0i} in (1), is [15]

$$\overline{X_2(k)} = N_A \sum_{i=1}^{K} \rho_i \delta(k - k_{0i}). \tag{3}$$

The variance at the frequency (cross-range) position k where there is no rigid body component is

$$\sigma_N^2 = \text{var}\{X_2(k)\} = N_A \frac{N - N_A}{N - 1} \sum_{i=1}^{K} \rho_i^2 = N_A \frac{N - N_A}{N - 1} E_x, \tag{4}$$

where $E_x = \sum_{i=1}^{K} \rho_i^2 = \frac{1}{N_A} \sum_{n \in \mathbb{N}_A} |x_{rb}(n)|^2$. For the detection of a signal component, the crucial parameter is

$$\frac{\sigma_N}{\left|\overline{X_2(k_i)}\right|} = \sqrt{\frac{N - N_A}{N_A (N - 1)}} \frac{\sqrt{E_x}}{|\rho_i|} \geq \sqrt{\frac{N - N_A}{N_A (N - 1)}}.$$

It is interesting to note that this relation corresponds to the Welch bound for the coherence (defining the maximal sparsity in the reconstruction).

The variance at a position of the signal's i-th component is

$$\sigma_{S_i}^2 = N_A \frac{N - N_A}{N - 1} \sum_{l=1, l \neq i}^{K} \rho_l^2.$$

According to the central limit theorem, the real and imaginary parts of the transform value for non-signal component (noise only) can be described by Gaussian distribution, $\mathcal{N}(0, \sigma_N^2/2)$ with zero-mean and variance σ_N^2. The probability density function for the absolute transform values outside signal components is Rayleigh-distributed [12]. The transform at a noise only position takes a value greater than Ξ, with probability

$$Q(\Xi) = \int_{\Xi}^{\infty} \frac{2\xi}{\sigma_N^2} e^{-\xi^2/\sigma_N^2} d\xi = \exp(-\frac{\Xi^2}{\sigma_N^2}). \tag{5}$$

Real and imaginary parts of the signal transform value, at the i-th signal component position, can be described by the Gaussian distributions

$$\mathcal{N}(N_A \rho_i, \sigma_{S_i}^2/2), \qquad \mathcal{N}(0, \sigma_{S_i}^2/2), \tag{6}$$

respectively. A real-valued ρ_i is assumed without any loss of generality. The probability density function (pdf) for the absolute transform values at the position of the i-th signal component, is Rice-distributed

$$p(\xi) = \frac{2\xi}{\sigma_{S_i}^2} e^{-(\xi^2 + \rho_i^2 N_A^2)/\sigma_{S_i}^2} I_0(\rho_i N_A 2\xi/\sigma_{S_i}^2), \xi \geq 0. \tag{7}$$

where I_0 is the zero-order modified Bessel function.

The probability that the Fourier transform of noise-alone is lower than Ξ is $[1 - Q(\Xi)]$. The total number of noise-only points is $M_K = N - K$, where K is the number of non-zero signal points. The probability that M_K independent transform noise-alone values are lower than Ξ is $[1 - Q(\Xi)]^{M_K}$. Probability that at least one of M_K transform noise-only values is greater than Ξ, is $G(\Xi) = 1 - [1 - Q(\Xi)]^{M_K}$. When a noise-only transform value surpasses the transform signal value, then

an error in the component detection occurs. To calculate this probability, consider the absolute transform value of a signal component at and around ξ. The transforms signal value is within ξ and $\xi + d\xi$ with the probability $p(\xi)d\xi$, where $p(\xi)$ is defined by (7). The probability that at least one of M_K noise-only transform values is above ξ can be written as

$$G(\xi) = 1 - [1 - Q(\xi)]^{M_K} . \tag{8}$$

Thus, the probability that the absolute transform signal component value is within the interval ξ, $\xi + d\xi$ and that at least one of the absolute transform noise-only values (outside the positions of the transform signal value) exceeds the transform signal value is $G(\xi)p(\xi)d\xi$. Considering all possible values of ξ, from (5) and (8), it follows that the probability of the wrong detection of the ith signal component is

$$P_{E_i} = \int_0^\infty G(\xi)p(\xi)d\xi \tag{9}$$

The approximation of this expression can be calculated by assuming that the transform of the i-th signal component is not random and that it is equal to $N_A\rho_i$ (positioned at the mean value of the signal's transform). This approximation assumes that the influence of noise to amplitude is symmetric. The form of error probability is then very simple

$$P_{E_i} \cong 1 - \left[1 - \exp(-\frac{N_A^2\rho_i^2}{\sigma_N^2})\right]^{M_K} . \tag{10}$$

This expression can be easily used for simple rough approximate analysis [12].

III. Statistical Case Study

The presented theory is tested and illustrated on a case study with a three-component rigid body signal

$$x(n) = \rho_1 e^{j2\pi k_{01} n/N} + \rho_2 e^{j2\pi k_{02} n/N} + \rho_3 e^{j2\pi k_{03} n/N}$$

with $\rho_1 = 0.75$, $\rho_2 = 1$, and $\rho_3 = 1.25$. Frequencies k_{01}, k_{02}, and k_{03} are chosen randomly from 0 to $N-1$ in each realization. No assumption about the distance of the components is done.

Since the presented recovery method will produce a correct result when the component positions (frequencies) are correctly detected in the initial estimation, analysis and comparison of the results and methods is done based on the wrong detection in the initial STFT calculation. Since there are three signal components in this example, the largest three values in the initial DFT are found based on the STFT and their positions are compared with the true frequencies k_{01}, k_{02}, and k_{03}. There are four possible outcomes:

1) The largest three values in the initial transform are at the positions of the signal components. Then, all signal components are detected and there is no wrong component detection.

2) Only two out of three largest values in the initial transform correspond to the signal frequencies. Then, there is one wrongly detected component. Probability of the event that one component is not detected among the largest three initial values will be denoted by $P(1)$.

3) Only one out of the three largest values in the initial transform corresponds to a signal frequency. In this case, there are two wrongly detected components. Probability of this event will be denoted by $P(2)$.

4) The three largest values in the initial estimation do not correspond to any of the signal component frequencies k_{01}, k_{02}, k_{03}. Then there are three wrongly detected components. Probability of this event is denoted by $P(3)$.

The average number of wrongly detected components is

$$N_E = 1P(1) + 2P(2) + 3P(3).$$

The number of wrongly detected components in percent is calculated as $N_{WD}[\%] = N_E/3 \times 100$. Division by 3 is done so that the maximal number of wrongly detected components, in this case 3, corresponds to 100 in percent.

In order to calculate the expected number of wrong detections, probabilities $P(1)$, $P(2)$ and $P(3)$ should be calculated using the derived expressions (9) or (10). The percent of wrongly detected maxima is statistically obtained and compared with the theoretical results. The statistically obtained results (percent of wrong detections as function of percent of missing samples) are presented by a solid green line in Fig.4. The theoretical results are presented by a solid red line, while the results obtained by using approximate error analysis are given by a red dotted line in Fig.4a) and Fig.4b).

Since the amplitudes of components differ, the wrong detection probabilities $P(1)$, $P(2)$ and $P(3)$ are calculated in the following way. Probability $P(1)$ is equal to the probability that at least one DFT sample corresponding to noise-only is greater than the DFT of the lowest component (P_{E1}) and that at the same time no other noise-only component is greater than the second largest signal component ($1 - P_{E2}$). This probability is

$$P(1) \cong P_{E1}(1 - P_{E2}).$$

Probabilities P_{E_1} and P_{E_2} are calculated according to (9) (or its approximation (10)). Here, the approximation sign is used instead of equality sign since we have neglected the probability that a single noise DFT value is greater than both the first (A_1) and the second (A_2) lowest signal DFT component. In other words, it has been assumed that the noise due to the missing samples is distributed in such a way that if one noise value surpasses the second largest component A_2, then there will be at least one additional noise component which is above the lowest signal component A_1.

Probability that: (a) at least one noise DFT value is greater than the third signal component (A_3), and that (b) at least one noise value is greater than the second component (A_2), and that (c) at least one noise component is greater than the first component (A_1), producing all three wrong positions of frequencies, is

$$P(3) \cong P_{E1}P_{E2}P_{E3}.$$

Similarly, the probability that there are two wrong detections is approximated by the probability that there is at least one noise component above the lowest signal component (equal to P_{E1}) and at the same time there is at least one noise component above the second signal component (equal to P_{E2}). There should be no noise component above the strongest signal value ($1 - P_{E3}$) as well. This probability is

$$P(2) \cong P_{E1}P_{E2}(1 - P_{E3}).$$

Here, similar approximations like in the case of $P(1)$ calculations are done.

Based on the previous results, the total average number of wrongly detected components is

$$N_E = P(1) + 2P(2) + 3P(3) \cong P_{E1} + P_{E1}P_{E2} + P_{E1}P_{E2}P_{E2}$$

with $N_{WD}[\%] = N_E/3 \times 100$ being a percent of the mean number of wrongly detected components and P_{E_i} ($i = 1, 2, 3$) are calculated according to (9) or its approximation (10).

In order to illustrate the previous effects on the reconstruction process, a single realization of a signal disturbed in the time-frequency domain is presented in Fig.3 with a small number of samples $N = 64$ and $M = 8$. The STFT of noisy (disturbed) signal is presented (top), along with the signal's DFT (radar image) in Fig.3a). The CS theory based reconstruction, after all disturbed samples are removed in the time domain, is shown in Fig.3b). The initial (norm-two or L-estimation) reconstruction, when all disturbed STFT values are just omitted, for this single realization is shown in Fig.3c). Reconstruction based on the

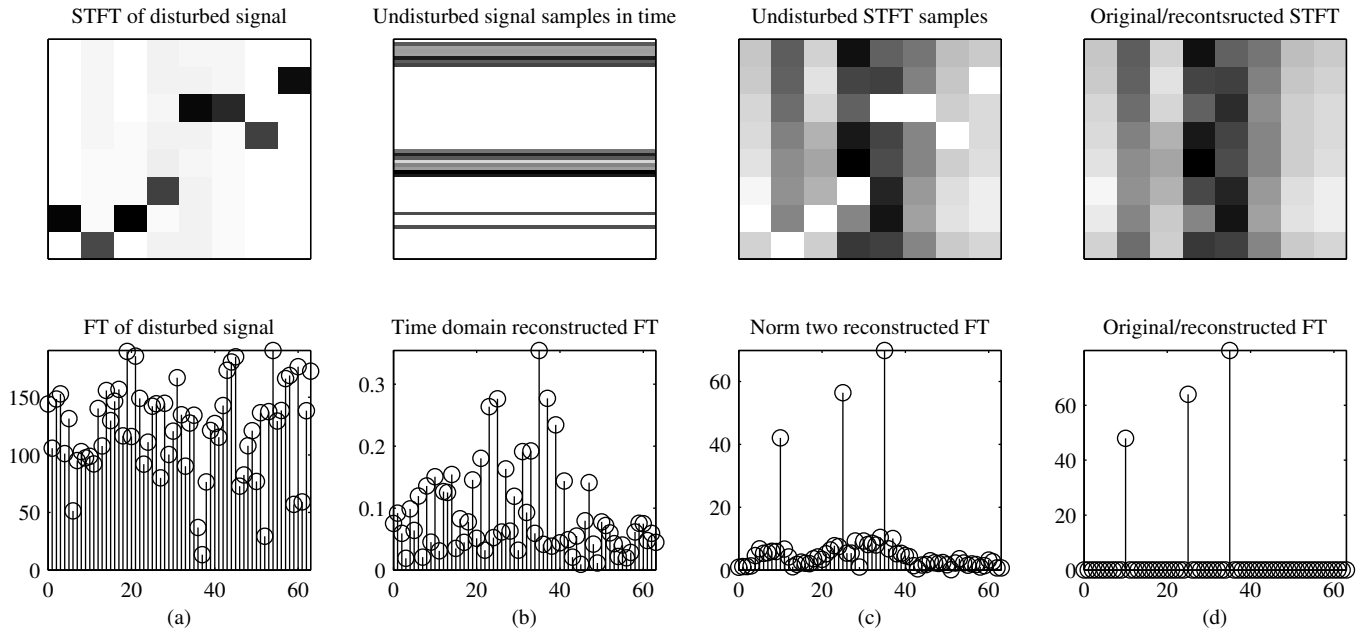

Fig. 3. A single realization illustration with $N = 64$, $M = 8$ and: (a) Signal with samples disturbed at arbitrary positions in the TF domain, (b) Signal with all disturbed samples removed in the time domain, (c) Signals with the disturbed samples removed in the TF domain, (d) Original/reconstructed signal.

presented method in the time-frequency domain results with the original DFT values, corresponding to undisturbed original rigid body image, presented in Fig.3d). Here we may conclude that a strong disturbance (corresponding to a micro-Doppler effect) completely masks the rigid body components in Fig.3a). Since the disturbance occurs in most of the time domain instants, then time domain analysis does not improve the results, Fig.3b). After the disturbed samples are removed then the norm-two based reconstruction is done, setting all disturbed samples to zero. Normalized reconstructed values are shown in Fig.3c). The norm-two reconstruction result is used in the described CS based reconstruction to get the reconstructed signal equal to the original signal Fig.3d). Next, a statistical analysis is described and performed with various numbers of missing STFT values.

A set of 100 random realizations of the signal and disturbance is used for averaging. In the DFT case (special case when the STFT reduces to the signal itself, $M = 1$), the results for wrong detection, as function of the percent of removed/unavailable samples, are presented in Fig.4a) for $N = 256$. In the case of the STFT, with $M = 2$, the results for wrong detection are presented in Fig.4b). The statistically obtained results are presented by a dashed blue line. The analysis based on the equivalent number of available samples in the time domain (2) is presented by a red line (solid red line for exact expression for the error probability and dotted red line for the approximate error expression). Matching with statistical results is high. The wrong detection percent if the STFT values (time-frequency domain) are omitted is presented by a solid green line. The analysis is repeated with different values of the window width M and the results are presented in Fig.4c)-d). It can be seen that for the omitted samples which are highly concentrated in the time-frequency domain their influence on the reconstruction (solid green lines) is low, while they significantly degrades performance of the time domain analysis (dashed blue lines) in Fig.4a)-d). The analysis has been performed using the nonoverlapping STFT calculation without assuming distant rigid body components. According to theoretical consideration in Section III, an additional STFT performance improvement can be achieved by using either the overlapping STFT calculation or assuming that the components may not be very close to each other.

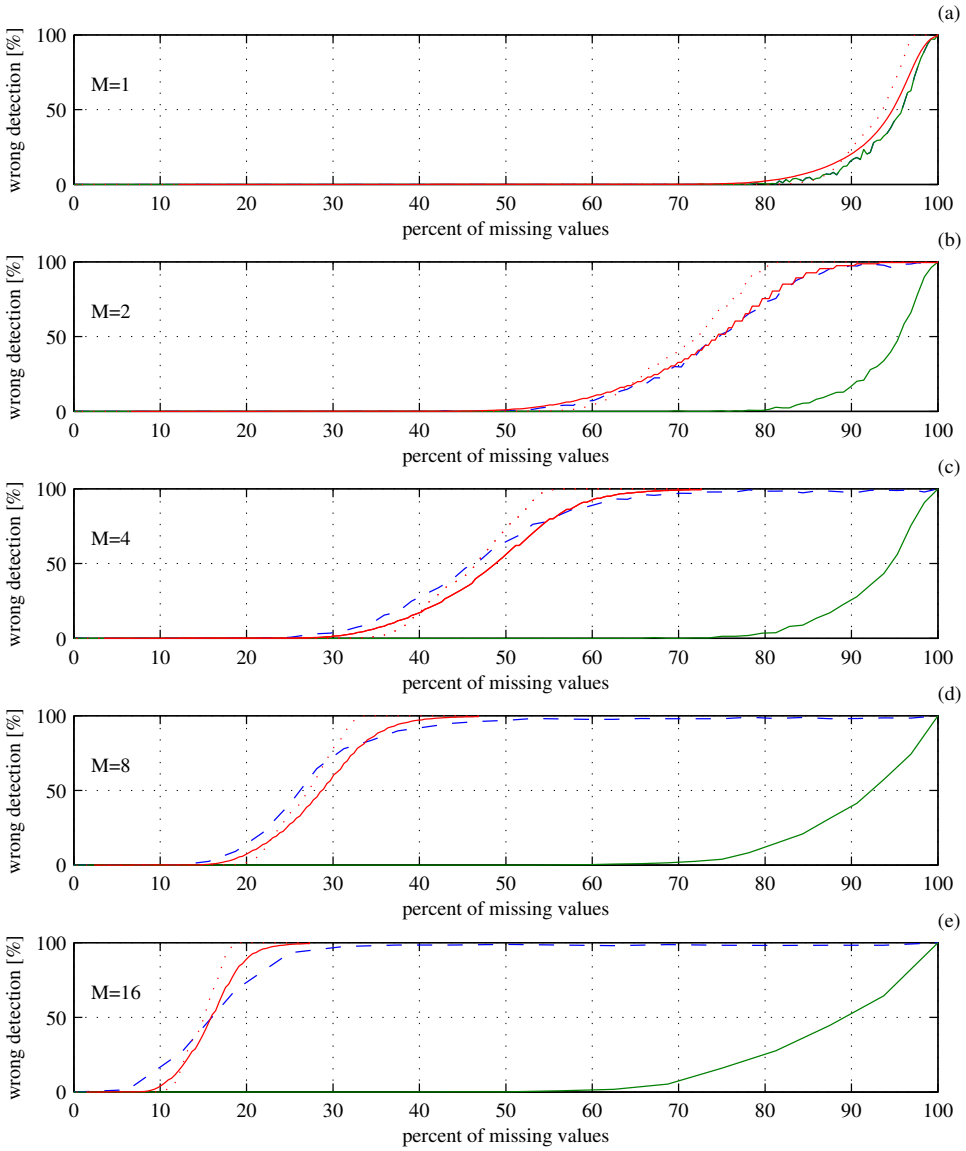

Fig. 4. An average number of wrongly detected components (in percent) for $N = 256$: (a) Signal in time ($M = 1$), (b) The TF analysis with $M = 2$, (c) The TF analysis with $M = 4$, (d) The TF analysis with $M = 8$, (e) The TF analysis with $M = 16$. The statistically obtained results using TF analysis are presented by solid green lines. The statistically obtained results by using time domain analysis are presented by dashed blue lines. The results obtained by the theory are presented by a solid red line, while the results obtained by using approximative error analysis are given by a red dotted line.

The worst case for the time domain (or frequency domain) analysis would be when the disturbances is well concentrated in time-frequency, but cover all the time and frequency interval. This case appears in some applications, like for example when a rigid body signal is disturbed by a simple linear frequency modulated (FM) or a sinusoidally modulated signal caused by a micro-Doppler effect. In these practically interesting examples, an analysis in the time (or in the frequency) domain would be almost impossible if the disturbance is high. The presented time-frequency based improvement will be even greater in these practical cases than in the statistical analysis presented in this section (where random positions of the disturbances in the time-frequency domain are assumed). Random positions allow a possibility that some or all of disturbances occupy only one time interval, while in practice even a small percentage of time-frequency disturbed area could spread over all time and frequency range and make the reconstruction impossible.

IV. Conclusion

The compressive sensing methods for the rigid body recovery are presented in the first part of this two-part paper, considering the micro-Doppler and rigid body separation. Since the compressive sensing theory produces quite conservative bounds for engineering applications, a statistical approach to the reconstruction from a reduced set of samples in the time-frequency domain is presented in this part of the paper. The approach is illustrated in a case study example. It shows that the full recovery results may be expected with high probability, well bellow the theoretical bounds, which include some zero probability events. One such event is described in the Appendix.

V. Appendix

As an illustration, consider the DFT of a signal with $N = 1024$ samples. If just one sample is missing and the number of available samples is $N_A = N - 1$ then the DFT reconstitution matrix is an equiangular tight frame with the exact condition for the signal reconstruction given by

$$K < \frac{1}{2}\left(1 + \sqrt{\frac{N - N_A}{N_A\,(N-1)}}\right) = N/2 = 512$$

nonzero DFT values. Assume that the missing sample is $x_{rb}(q)$ and that its value has to be reconstructed. Consider a rigid body signal with sparsity K

$$x_{rb}(n) = \sum_{i=1}^{K} \rho_i e^{j2\pi k_{0i} n/N}.$$

The signal reconstruction is based on $x_0(n) = x_{rb}(n) + z\delta(n-q)$ where z indicates arbitrary deviation from the unknown value of $x_{rb}(n)$. The DFT of the signal $x_0(n)$ is

$$X_0(k) = N\sum_{i=1}^{K} \rho_i \delta(k - k_{0i}) + z e^{-j2\pi kq/N}.$$

Using the norm-zero definition, we get the number of non-zero DFT values as

$$\|\mathbf{X}_0\|_0 = \sum_{k=0}^{N-1} |X_0(k)|^0 = \sum_{i=1}^{K} \left|N\rho_i + z e^{-j2\pi k_{0i} q/N}\right|^0 + \sum_{i=K+1}^{N} |z|^0$$

Obviously

$$\|\mathbf{X}_0\|_0 = \begin{cases} N & \text{for} \quad |z| \neq 0 \text{ and } z \neq -N\rho_i e^{j2\pi k_{0i} q/N} \text{ for any } i \\ N-1 & \text{for} \quad |z| \neq 0 \text{ and } z = -N\rho_i e^{j2\pi k_{0i} q/N} \text{ only for one } i \\ .. & .. \quad\quad ... \\ N-P & \text{for} \quad |z| \neq 0 \text{ and } z = -N\rho_i e^{j2\pi k_{0i} q/N} \text{ for } P \text{ values of } i \\ N-K & \text{for} \quad |z| \neq 0 \text{ and } z = -N\rho_i e^{j2\pi k_{0i} q/N} = -NC \text{ for all } i = 1,..,K \\ K & \text{for} \quad |z| = 0. \end{cases}$$

With just one missing (eliminated) value minimum of $\|\mathbf{X}_0\|_0$ is achieved for $z = 0$ only if $K < N - K$, i.e. $K < N/2$.

From the previous equation, we see that for $K = N/2$, the last two rows will produce the same result $N - K = N/2$ and $K = N/2$. In that case the minimum of $\|\mathbf{X}_0\|_0$ can not produce unique solution. The condition $\|\mathbf{X}_0\|_0 = N - K$ also requires

$$\rho_1 e^{j2\pi k_{01} q/N} = \rho_2 e^{j2\pi k_{02} q/N} = \rho_3 e^{j2\pi k_{03} q/N} = ... = \rho_K e^{j2\pi k_{0K} q/N} = C$$

In reality the case that $K = 512$ reflection coefficients have equal amplitude

$$|\rho_1| = |\rho_2| = |\rho_3| = ... = |\rho_K|$$

and that at the same time the missing sample position q is such that

$$\arg\{\rho_1\} + 2\pi k_{01}q/N = \arg\{\rho_2\} + 2\pi k_{02}q/N = ... = \arg\{\rho_K\} + 2\pi k_{0K}q/N \tag{11}$$

is a zero probability event of the second order. It can be neglected or treated as singular case. Thus, one missing sample allows reconstruction with values of $K = N/2$, with probability close to one.

This singularity can also be explained in an illustrative way. Consider the DFT transform $X_0(k)$ of the singular case $\rho_1 = \rho_2 = \rho_3 = ... = \rho_K = C$ with zero phases of all ρ_i. According to (11), the critical case is when the missing sample is $x_{rb}(0)$ with $q = 0$ since k_{0i} are random values not equal to each other. The DFT in this (second order) zero-probability event case is

$$X_0(k) = \sum_{i=1}^{K} NC\delta(k - k_{0i}) + z.$$

It is a comb of equal values at $K = N/2$ frequencies $k = k_{0i}$. By using $z = -NC$, we cancel out all DFT values at $k = k_{0i}$ however introduce new DFT values $-NC$ at $k \neq k_{0i}$. These two DFTs are complementary to each other, but have the same sparsity.

If $K > N/2$ with $\rho_1 = \rho_2 = \rho_3 = ... = \rho_K = C$, in the same way we can easily conclude that $\|\mathbf{X}_0\|_0$ will produce $z = -NC$ with sparsity $N - K < N/2$. However, it is not a signal we intended to recover.

The analysis can easily be generalized to a signal with $Q = N - M$ missing samples.

REFERENCES

[1] Chen, V.C., Tahmoush, D., and Miceli, W.J.: 'Radar Micro-Doppler Signatures: Processing and Applications' (IET, 2014).

[2] Stanković, L., Daković, M., Thayaparan, T., and Popović-Bugarin, V.: 'Micro-Doppler Removal in the Radar Imaging Analysis', IEEE Transactions on Aerospace and Electronic Systems, 2013, **49**, (2), pp 1234–1250.

[3] Totir, F., and Radoi, E.: 'Superresolution algorithms for spatial extended scattering centers', Digital Signal Processing, 2009, **19**, (5), pp 780–792

[4] Chen, V.C., Li, F., Ho, S.S., and Wechsler, H.: 'Micro-Doppler effect in radar: phenomenon, model, and simulation study', IEEE Transactions on Aerospace and Electronic Systems, 2006, **42**, (1), pp 2–21

[5] Martorella, M.: 'Novel approach for ISAR image cross-range scaling', IEEE Trans. Aerosp. Electron. Syst., 2008, **44**, (1), pp 281–294

[6] Wang, Y., Ling, H., and Chen, V.C.: 'ISAR motion compensation via adaptive joint time-frequency techniques', IEEE Transactions on Aerospace and Electronic Systems, 1998, **38**, (2), pp 670–677

[7] Sparr, T., Krane, B.: 'Micro-Doppler analysis of vibrating targets in SAR', IEE Proc. Radar Sonar Navig., 2003, **150**, (4), pp 277–283

[8] Thayaparan, T., Abrol, S., Riseborough, E., Stanković, L., Lamothe, D., and Duff, G.: 'Analysis of radar micro-Doppler signatures from experimental helicopter and human data', IET Proceedings Radar Sonar and Navigation, 2007, **1**, (4), pp 288–299

[9] Chen, V.C., Ling, H.: 'Time-frequency transforms for radar imaging and signal analysis' (Artech House, Boston, 2002)

[10] Stanković, L., Daković, M., and Thayaparan, T.: 'Time-Frequency Signal Analysis with Applications', (Artech House, Boston, 2013).

[11] Stanković, L., Thayaparan, T., and Djurović, I.: 'Separation of target rigid body and micro-Doppler effects in ISAR imaging', IEEE Transactions on Aerospace and Electronic Systems, 2006, **41**, (4), pp 1496–1506

[12] Stanković, L., Stanković, S., and Amin, M.: 'Missing Samples Analysis in Signals for Applications to L-Estimation and Compressive Sensing', Signal Processing, 2014, **94**, pp 401–408

[13] Stanković, L., Stanković, S., Orović, I., and Amin, M.: 'Compressive Sensing Based Separation of Non-Stationary and Stationary Signals Overlapping in Time-Frequency', IEEE Transactions on Signal Processing, 2013, **61**, (18), pp 4562–4572

[14] Donoho, D.: 'Compressed sensing', IEEE Transactions on Information Theory, 2006, **52**, (4), pp 1289–1306.

[15] Stanković, L., Stanković, S., Daković, M., and Orović, I.: 'Separation and Reconstruction of the Rigid Body and Micro-Doppler Signal in ISAR: Part I – Theory', IET Radar, Sonar and Navigation, Special Issue: Micro Doppler